

# Reconfigurable Intelligent Surface-Enabled Spectrum-Sharing Communications Based on Successive Interference Cancellation

Weiye Chen, Haiyang Ding, *Member, IEEE*, Shilian Wang, *Member, IEEE*, Fengkui Gong,  
and Pedro Henrique Juliano Nardelli, *Senior Member, IEEE*

**Abstract**—In this letter, a reconfigurable intelligent surface (RIS)-enabled successive interference cancellation (SIC)-based spectrum sharing (SS) scheme is proposed for SS networks where multiple transceiver pairs use the same spectrum at the same time. The key idea is to apply the SIC technique at each receiver and utilize RIS simultaneously, so as to reduce the interference among different transceiver pairs and to focus energy. Specifically, to minimize the total power consumption at all the transmitters under given data rate constraints, the decoding order at each receiver, the reflection coefficients at RIS, and the transmit power at each transmitter are jointly optimized. The formulated problem is a mixed-combinatorial-and-continuous optimization problem and thus is difficult to solve. To address this, a low-complexity but effective decoding order determining method is first proposed. Given the decoding orders, the reflection coefficients and the transmit power are alternately optimized with the help of the semidefinite relaxation method. Substantial performance gains are shown compared with traditional RIS-enabled SS scheme without SIC.

**Index Terms**—RIS, spectrum sharing, successive interference cancellation, non-convex optimization.

## I. INTRODUCTION

WITH the rapid development of Internet of Things (IoT) [1], wireless data traffic has shown an explosive growth, calling for more spectrums [2]. Many spectrum sharing techniques have been proposed to solve this problem, which include cognitive radio (CR) [3], ambient backscatter communications (AmBC) [4], and full-duplex (FD) communications [5]. However, the CR technique cannot provide reliable connections since the spectrum has to be vacated when the primary users reclaim it. The AmBC technique has limited transmission range due to the double fading effects, while the FD technique requires high-complexity hardware and introduces non-negligible residual loop self-interference.

Fortunately, by observing that the essence of spectrum sharing is to alleviate interference, an innovative and revolutionary technology developed in recent years, namely reconfigurable intelligent surface (RIS) [6], has been found to be a useful

alternative technique for spectrum sharing [7]. An RIS is a thin surface with a large number of low-cost nearly-passive programmable reflecting elements. By controlling the integrated circuits on RIS, the amplitude and/or phase of the incident electromagnetic waves can be modified to focus the signals' energy and/or to alleviate interference. Therefore, the RIS technique can be utilized to facilitate multiple transceiver pairs to use the same spectrum simultaneously. In this regard, the work in [7] considered an RIS-aided device-to-device network with one base station-to-user single-input-single-output (SISO) link and  $D$  device-to-device SISO links, which can be regarded as  $(D + 1)$  transceiver pairs who occupy the same spectrum. In particular, the work in [7] has shown that the RIS can indeed focus the energy of the transmitted signals to their corresponding receivers and meanwhile reduce the interference among different transceiver pairs, which helps boost the spectrum efficiency.

Even with RIS, the interference among different transceiver pairs may not be completely alleviated. The work in the field of power-domain non-orthogonal multiple access (NOMA) [8] inspired us to further alleviate the interference by using successive interference cancellation (SIC) in RIS-enabled spectrum sharing networks (RIS-SSN) with multiple transceiver pairs, which has not been considered yet in existing works. The key idea of SIC is to allow receivers to firstly recover the information from unintended but strong signals, then remove these signals from their observations, and finally recover their own information. In this way, the negative impacts of interference can be reduced significantly.

The major contributions of this letter are summarized as follows. To begin with, for SSN with multiple transceiver pairs, an RIS-enabled SIC-based spectrum sharing (RIS-SIC-SS) scheme is proposed, which utilizes the SIC technique and RIS at the same time to reduce the interference among different transceiver pairs. Then, the decoding order at each receiver, the reflection coefficients at RIS, and the transmit power at each transmitter are jointly optimized to reduce the total power consumption at all the transmitters under given data rate constraints. To address the formulated mixed-combinatorial-and-continuous problem, a low-complexity decoding order determining method is first proposed. Given the decoding orders, the reflection coefficients and the transmit power are alternately optimized with the help of the semidefinite relaxation (SDR) method. Simulation results show that the proposed scheme can effectively reduce the interference and

W. Chen and S. Wang are with College of Electronic Science and Technology, National University of Defense Technology, Changsha, China (email: chenweiye14@nudt.edu.cn, wangsl@nudt.edu.cn).

H. Ding is with College of Information and Communication, National University of Defense Technology, Xi'an, China (email: dinghy2003@hotmail.com).

F. Gong is with the State Key Laboratory of Integrated Service Networks, Xidian University, Xi'an, China (e-mail: fkgong@xidian.edu.cn).

P. H. J. Nardelli is with the School of Energy Systems, Lappeenranta University of Technology, Lappeenranta, Finland (e-mail: Pedro.Nardelli@lut.fi).

Corresponding author: Shilian Wang.

allow more transceiver pairs to communicate over the same spectrum, even with less power consumption.

## II. SYSTEM MODEL AND PROBLEM FORMULATION

### A. System Model

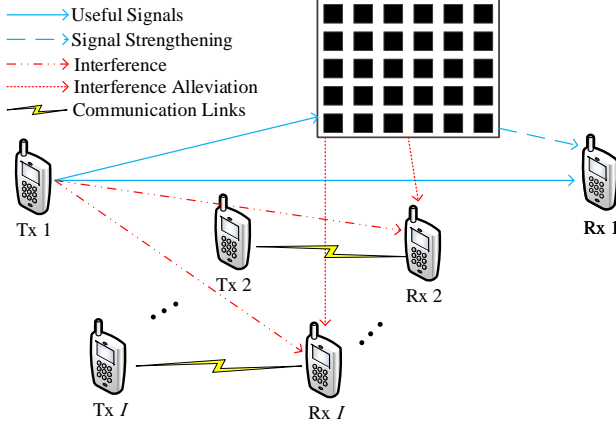


Fig. 1: RIS-enabled spectrum sharing network, where only the signals transmitted by transmitter 1 are explicitly plotted.

As shown in Fig. 1, we consider an RIS-SSN with  $I$  pairs of transceivers, who occupy the same spectrum simultaneously. Specifically, the data rate of the  $i$ -th transceiver pair is assumed to be  $R_i$ . An RIS consisting of  $N$  programmable elements is deployed to enhance the received desired signals and meanwhile to reduce the undesired interference at the receivers. Block fading channel model is considered, where channel coefficients remain unchanged within each transmission block, but may vary for different blocks. At least one transceiver is assumed to sustain full channel state information (CSI) to coordinate the network<sup>12</sup>.

Let  $\theta_n$  represents the reflection coefficient of the  $n$ -th element of the RIS, whose amplitude and phase are assumed to be one and continuously adjustable within  $[0, 2\pi]$ , respectively, as in [9]. We define  $\boldsymbol{\theta} \triangleq [\theta_1, \theta_2, \dots, \theta_N]^H$ . Then, the received signals at the  $i$ -th receiver can be written as

$$y_i = \sum_{j=1}^I \sqrt{P_j} (h_{j,i} + \boldsymbol{\theta}^H \mathbf{g}_{j,i}) x_j + n_i, \quad (1)$$

where  $x_j \sim \mathcal{CN}(0, 1)$  represents the transmitted symbols from the  $j$ -th transmitter,  $P_j$  denotes the corresponding transmit power,  $h_{j,i}$  indicates the channel coefficient of the direct link from the  $j$ -th transmitter to the  $i$ -th receiver,  $n_i$  represents the zero-mean additive white Gaussian noise at the  $i$ -th receiver with variance  $\sigma_i^2$ , and  $\mathbf{g}_{j,i} \triangleq [g_{j,1,i}, g_{j,2,i}, \dots, g_{j,N,i}]^T$  denotes the cascaded channel coefficients of the links from the  $j$ -th transmitter to the  $i$ -th receiver through the RIS elements.

<sup>1</sup>For example, one of the transceiver pairs could be an access point (AP) and its corresponding user, whereas the remaining transceiver pairs are sharing the same spectrum with the AP (i.e., device-to-device links) [7]. In this case, the AP has a relatively high processing ability for running the algorithm developed in this letter.

<sup>2</sup>Network coordination and channel estimations require additional communication overheads. However, as will be seen in Section IV, the proposed scheme can provide significant performance gains.

### B. RIS-SIC-SS Scheme

In previous work [7], the  $i$ -th receiver attempts to recover  $x_i$  by treating all the  $x_j$  ( $j \neq i$ ) as interference. However, if the received power of  $x_j$  at the  $i$ -th receiver (i.e.,  $P_j |h_{j,i} + \boldsymbol{\theta}^H \mathbf{g}_{j,i}|^2$ ) is much larger than that of  $x_i$  (i.e.,  $P_i |h_{i,i} + \boldsymbol{\theta}^H \mathbf{g}_{i,i}|^2$ ), the receiver can indeed use the SIC technique to recover  $x_j$  first, and then subtract  $x_j$  from its observations before recovering  $x_i$ . Therefore, in the proposed RIS-SIC-SS scheme, each receiver has its own decoding order, and we denote the decoding order of receiver  $i$  by  $\Lambda_i = \{D_{i1}, D_{i2}, \dots, i\}$ , whose elements are the indexes of the transmitters. Note that  $\Lambda_i$  has at least one element and the last element must be  $i$  since the goal of receiver  $i$  is to recover  $x_i$ . Next, let interference set  $\Pi_{j,i}$  represents the indexes of the interference signals at receiver  $i$  when it attempts to recover  $x_j$ . For instance, if there are four pairs of transceivers in total, and if the decoding order of the 3-rd receiver is  $\Lambda_3 = \{2, 1, 3\}$ , then we have  $\Pi_{2,3} = \{1, 3, 4\}$ ,  $\Pi_{1,3} = \{3, 4\}$  and  $\Pi_{3,3} = \{4\}$ .

### C. Problem Formulation

We aim to minimize the total power consumption by optimizing the transmit power at the transmitters (i.e.,  $\mathbf{P} \triangleq \{P_1, P_2, \dots, P_I\}$ ), the phase shifts  $\boldsymbol{\theta}$  at the RIS, and the decoding orders  $\boldsymbol{\Lambda} \triangleq \{\Lambda_1, \Lambda_2, \dots, \Lambda_I\}$ . Therefore, the problem can be written as

$$\begin{aligned} (\text{P1}) : & \min_{\mathbf{P}, \boldsymbol{\theta}, \boldsymbol{\Lambda}} \sum_{i=1}^I P_i \\ \text{s.t. (a)} & \log_2 \left( 1 + \frac{P_j |h_{j,i} + \boldsymbol{\theta}^H \mathbf{g}_{j,i}|^2}{\sum_{k \in \Pi_{j,i}} P_k |h_{k,i} + \boldsymbol{\theta}^H \mathbf{g}_{k,i}|^2 + \sigma_i^2} \right) \geq R_j, \\ & \forall j \in \Lambda_i, \forall i = 1, 2, 3, \dots, I, \\ \text{(b)} & |\theta_n| = 1, \forall n = 1, 2, 3, \dots, N, \\ \text{(c)} & P_i \geq 0, \forall i = 1, 2, 3, \dots, I, \end{aligned} \quad (2)$$

where constraint (a) indicates the signal-to-interference-plus-noise ratio (SINR) requirement at receiver  $i$  when it attempts to recover  $x_j$ .

## III. PROPOSED SOLUTIONS

### A. Determining Decoding Orders

It is worth mentioning that different from the works in [10]–[12], where downlink NOMA is considered, in the RIS-SSN considered in this letter, the relative strength of the received signals from different transmitters is generally different at different receivers since they experience different channel attenuations. This means that the optimal decoding orders at different receivers are generally different, which makes problem (P1) to be a complicated mixed-combinatorial-and-continuous optimization problem. One way to tackle this is to exhaustively search all the possible decoding orders and select the one which maximizes the objective function [10]. Another way is to heuristically select the decoding orders by simple computation [11], [12]. We choose the latter approach due to its low computational complexity, which is especially effective when the number of transceiver pairs is large. Specifically, for

receiver  $i$ , we firstly quantify its difficulty of recovering  $x_j$  by  $(2^{R_j} - 1) \frac{\sigma_i^2}{|h_{j,i}|^2}$ , which is indeed the minimum required transmit power at transmitter  $j$  when other transmitters and the RIS are ignored<sup>3</sup>. Then, each transmitter's information is arranged to be decoded ahead of those who are more difficult to recover. For example, for the 3-rd receiver, if  $\frac{(2^{R_2} - 1)}{|h_{2,3}|^2} < \frac{(2^{R_1} - 1)}{|h_{1,3}|^2} < \frac{(2^{R_3} - 1)}{|h_{3,3}|^2} < \frac{(2^{R_4} - 1)}{|h_{4,3}|^2}$ , we have  $\Lambda_3 = \{2, 1, 3\}$ .

Unfortunately, even with given decoding orders, the problem is still difficult to be solved since  $\theta$  and  $\mathbf{P}$  are strongly coupled in constraint (a) and also due to the non-convexity constraints (a) and (b). To solve this problem, we first note that constraint (b) only contains variable  $\theta$ , while constraint (c) only contains variable  $\mathbf{P}$ . This motivates us to solve the problem by optimizing  $\theta$  and  $\mathbf{P}$  alternately.

### B. Optimizing $\theta$ with Given $\mathbf{P}$

Note that the objective function does not contain  $\theta$ , and constraint (a) is the only inequality constraint related to  $\theta$ . Therefore, we optimize  $\theta$  to maximize the margin of constraint (a), which can be expressed as

$$s = \min_{\forall j \in \Lambda_i, \forall i=1,2,3,\dots,I} \left\{ \frac{P_j |h_{j,i} + \theta^H \mathbf{g}_{j,i}|^2}{(2^{R_j} - 1)} - \sum_{k \in \Pi_{j,i}} P_k |h_{k,i} + \theta^H \mathbf{g}_{k,i}|^2 - \sigma_i^2 \right\}. \quad (3)$$

To begin with, note that constraint (a) is not a convex constraint. To deal with this problem, we define  $\bar{\theta} \triangleq \begin{bmatrix} \theta \\ 1 \end{bmatrix}$ ,  $\Theta \triangleq \bar{\theta} \bar{\theta}^H$ , and  $\mathbf{S}_{j,i} \triangleq \begin{bmatrix} \mathbf{g}_{j,i} \mathbf{g}_{j,i}^H & \mathbf{g}_{j,i} h_{j,i}^H \\ h_{j,i} \mathbf{g}_{j,i}^H & 0 \end{bmatrix}$ . Based on these definitions, we have

$$|h_{j,i} + \theta^H \mathbf{g}_{j,i}|^2 = \bar{\theta}^H \mathbf{S}_{j,i} \bar{\theta} + |h_{j,i}|^2 = \text{Tr}(\mathbf{S}_{j,i} \Theta) + |h_{j,i}|^2. \quad (4)$$

By inserting (4) into constraint (a) and by applying the SDR method, the subproblem of optimizing  $\theta$  can be given by

$$\begin{aligned} (\text{P2-a}) : \max_{\Theta, s} & \\ \text{s.t. (a)} & \frac{P_j \left( \text{Tr}(\mathbf{S}_{j,i} \Theta) + |h_{j,i}|^2 \right)}{(2^{R_j} - 1)} - \sigma_i^2 \\ & - \sum_{k \in \Pi_{j,i}} P_k \left( \text{Tr}(\mathbf{S}_{k,i} \Theta) + |h_{k,i}|^2 \right) \geq s, \\ & \forall j \in \Lambda_i, \forall i = 1, 2, 3, \dots, I, \\ & (\text{b}) \Theta \succeq 0, \\ & (\text{c}) [\Theta]_{n,n} = 1, \forall n = 1, 2, 3, \dots, N+1, \end{aligned} \quad (5)$$

which is a convex problem and can be solved by the CVX tool. Generally, the optimal  $\Theta^*$  obtained by solving (P2-a) is not rank-one. We use the Gaussian randomization method to obtain a rank-one solution [12]. To be more specific, we

first compute the eigenvalue decomposition of  $\Theta^*$  as  $\Theta^* = \mathbf{U} \Sigma \mathbf{U}^H$ , and then generate random vectors  $\bar{\theta}_r = \mathbf{U} \Sigma^{\frac{1}{2}} \mathbf{r}$ , where  $\mathbf{r} \sim \mathcal{CN}(\mathbf{0}, \mathbf{I}_{N+1})$ . Next, the reflection coefficients are generated as  $\theta_r = e^{j \angle(\bar{\theta}_r(1:N) / \bar{\theta}_r(N+1))}$ , where  $\bar{\theta}_r(1:N)$  represents the first  $N$  elements in  $\bar{\theta}_r$  and  $\bar{\theta}_r(N+1)$  indicates the  $(N+1)$ -th element of  $\bar{\theta}_r$ . Finally, the best  $\theta_r$  that maximizes (3) is selected as the optimization result  $\theta^*$ .

### C. Optimizing $\mathbf{P}$ with Given $\theta$

With given  $\theta$  and given decoding orders, (P1) is reduced to

$$\begin{aligned} (\text{P2-b}) : \min_{\mathbf{P}} & \sum_{i=1}^I P_i \\ \text{s.t. (a)} & \frac{P_j |h_{j,i} + \theta^H \mathbf{g}_{j,i}|^2}{(2^{R_j} - 1)} - \sum_{k \in \Pi_{j,i}} P_k |h_{k,i} + \theta^H \mathbf{g}_{k,i}|^2 - \sigma_i^2 \\ & \geq 0, \forall j \in \Lambda_i, \forall i = 1, 2, 3, \dots, I, \\ & (\text{b}) P_i \geq 0, \forall i = 1, 2, 3, \dots, I, \end{aligned} \quad (6)$$

which is a convex optimization problem and can be readily solved by the CVX tool.

### D. Overall Algorithm

Before iteratively optimizing  $\theta$  and  $\mathbf{P}$  to minimize the power consumption, we have to find a feasible solution as a start point, which can be done by alternately optimizing  $\theta$  by solving (P2-a) and  $\mathbf{P}$  by solving the following margin maximization problem:

$$\begin{aligned} (\text{P2-c}) : \max_{\mathbf{P}, s} & s \\ \text{s.t. (a)} & \frac{P_j |h_{j,i} + \theta^H \mathbf{g}_{j,i}|^2}{(2^{R_j} - 1)} - \sum_{k \in \Pi_{j,i}} P_k |h_{k,i} + \theta^H \mathbf{g}_{k,i}|^2 - \sigma_i^2 \\ & \geq s, \forall j \in \Lambda_i, \forall i = 1, 2, 3, \dots, I, \\ & (\text{b}) P_i \geq 0, \forall i = 1, 2, 3, \dots, I, \\ & (\text{c}) P_i \leq P_{\max}, \forall i = 1, 2, 3, \dots, I, \end{aligned} \quad (7)$$

where constraint (c) is added to prevent the optimization result to be infinity, and  $P_{\max}$  is set to be sufficient large to avoid losing feasible solutions.

The proposed algorithm is summarized in Algorithm 1, where steps 2~15 are used to find a feasible solution, while steps 16~21 stand for the power consumption minimization process.

### E. Convergence and Computational Complexity

Since the objective function  $\sum_{i=1}^I P_i$  is non-increasing over iterations and is bounded from below by zero, Algorithm 1 is guaranteed to converge [9]. In what follows, we analyze the computational complexity of Algorithm 1, which is mainly due to step 8 because each time we generate a  $\theta_r$  based on Gaussian randomization, equation (3) has to be used once to evaluate its performance. To begin with, note that there are  $I$  decoding order sets (i.e.,  $\Lambda_i$ ) in total. In worst case, each  $\Lambda_i$  has  $I$  elements in total. In this case, for given index  $i$  and for  $I$  different indexes  $j$  (i.e.,  $j = 1, 2, \dots, I$ ),  $\Pi_{j,i}$

<sup>3</sup>Herein, although the impacts of the transmitter-RIS-receiver links are ignored, the reflection coefficients at RIS can be adjusted to reform the transmitter-RIS-receiver links to fit the adopted decoding orders.

---

**Algorithm 1** Power Consumption Minimization Algorithm
 

---

- 1: Initialize the optimal value and the iteration times of margin maximization problem  $s^t = -\infty$  and  $t_M = 0$ , respectively. Set maximum allowed solving times  $N_M$  for margin maximization problem, Gaussian randomization times  $N_G$ , convergence tolerance  $\epsilon$ , and initial transmit power  $P_i^t = P_{\text{initial}}, \forall i = 1, 2, \dots, I$
  - 2: **repeat**
  - 3:   **if** ( $t_M > N_M$ ) **then**
  - 4:     **return** Unfeasible
  - 5:   **else**
  - 6:     Update iteration times  $t_M = t_M + 1$
  - 7:     Find optimal  $\Theta^{t+1}$  by solving (P2-a) with given  $P^t$
  - 8:     Use Gaussian randomization method for  $N_G$  times based on  $\Theta^{t+1}$  to find the maximum margin  $s^{t+1}$  and the corresponding  $\theta^{t+1}$  by using (3)
  - 9:     **if** ( $s^{t+1} > s^t$ ) **then**
  - 10:       Update  $s^t = s^{t+1}; \theta^t = \theta^{t+1}$
  - 11:     **end if**
  - 12:     Find optimal  $P^{t+1}$  and  $s^{t+1}$  by solving (P2-c) with given  $\theta^t$
  - 13:     Update  $s^t = s^{t+1}; P^t = P^{t+1}$
  - 14:   **end if**
  - 15: **until**  $s^t > 0$
  - 16: **repeat**
  - 17:   Update  $P^t = P^{t+1}$
  - 18:   Update  $s^t$  based on  $\theta^t$  and  $P^t$  by using equation (3)
  - 19:   Execute step 7~11
  - 20:   Find optimal  $P^{t+1}$  by solving (P2-b) with given  $\theta^t$
  - 21: **until**  $\text{sum}(P^t) - \text{sum}(P^{t+1}) < \epsilon$
  - 22: **return**  $\theta^* = \theta^t, P^* = P^{t+1}$
- 

has  $0, 1, 2, 3, \dots, I - 1$  elements in total, respectively. As a result, equation (3) contains  $I^2 \times (\frac{I-1}{2} + 1) \approx \frac{I^3}{2}$  terms like  $P_j |h_{j,i} + \theta^H g_{j,i}|^2$ , whose computational complexity mainly comes from the terms like  $\theta^H g_{j,i}$ . Since the computational complexity of  $\theta^H g_{j,i}$  is mainly due to  $(N + 1)$  times of multiplication, we can conclude that the computational complexity of Algorithm 1 can be written as  $O(I^3 \times (N + 1))$  in the worst case. On the contrary, in the best case, each  $\Lambda_i$  only contains one element (i.e.,  $i$ ), and each corresponding  $\Pi_{i,i}$  has  $(I - 1)$  elements. In a similar way, we can conclude that the computational complexity of Algorithm 1 can be written as  $O(I^2 \times (N + 1))$  in the best case.

#### IV. NUMERICAL RESULTS AND DISCUSSION

In this section, we compare the performance of the proposed RIS-SIC-SS scheme with that of the RIS-SSN without SIC [7]. The latter scheme is named as benchmark scheme in the rest of the letter. For fair comparison, Algorithm 1 is adopted for both schemes in the simulations. The only difference between them is the adopted decoding orders. Additionally, the SIC-based SSN without RIS and the pure SSN without using either techniques are also considered by setting the number of the RIS elements in the proposed scheme and that of the benchmark scheme to zero, respectively. Two metrics

are considered. They are the feasible rate and the average power consumption per transceiver pair. The feasible rate is defined as the probability that the result of the margin maximization problem is positive (i.e., a feasible solution can be found) and, equivalently, all the receivers can recover their desired information<sup>4</sup>. The average power consumption per transceiver pair is defined as the average total power consumption (in feasible transmission blocks) divided by the number of transceiver pairs.

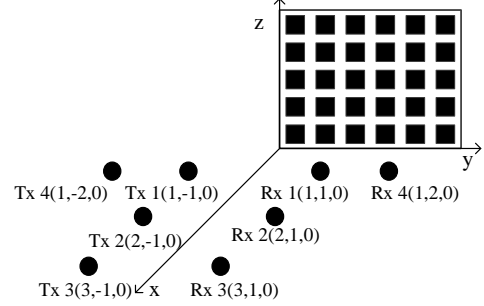


Fig. 2: The considered Cartesian coordinate.

As shown in Fig. 2, we use a three dimensional Cartesian coordinate to represent the positions of communication nodes, where a rectangular RIS is placed in the Y-Z plane with its origin located at the bottom left corner of the RIS, and the Y-axis and the Z-axis as the alignment edges [7]. Without loss of generality, at most four transceiver pairs are considered. The coordinates of the transmitters are  $(1, -1, 0)$ ,  $(2, -1, 0)$ ,  $(3, -1, 0)$ , and  $(1, -2, 0)$  in meter, respectively. The corresponding receivers are located at  $(1, 1, 0)$ ,  $(2, 1, 0)$ ,  $(3, 1, 0)$ , and  $(1, 2, 0)$  in meter, respectively. The distances between adjacent RIS elements are set to be half of the wave length and the wave length is set to be 0.3 meters. All the channels are modeled by Rayleigh fading. The average channel power gain between a transmitter and a receiver is calculated according to the Friis transmission equation with unit antenna gain, so is the average channel power gain between an RIS element and a transmitter/receiver. Unless otherwise specified, the simulation parameters setup is adopted as  $R_1 = R_2 = R_3 = R_4 = 1\text{bit/s/Hz}$ ,  $\sigma_1^2 = \sigma_2^2 = \sigma_3^2 = \sigma_4^2 = 5 \times 10^{-5}\text{W}$ ,  $\epsilon = 10^{-3}$ ,  $P_{\text{initial}} = 10\text{W}$ ,  $N_M = 5$ , and  $N_G = 1000$ . Each result is obtained by 2000 channel realizations.

Fig. 3 presents the feasible rate of the proposed RIS-SIC-SS scheme and that of the benchmark scheme. Several observations can be drawn as follows: 1) The proposed scheme significantly improves the feasible rate compared with the benchmark scheme. This is because the SIC technique helps alleviate interference, which facilitates the receivers to recover their desired information; 2) Even without RIS, applying the SIC technique can still significantly improve the feasible rate, compared with the pure SSN without using either techniques; 3) With the increase of the number of RIS elements, the feasible rate can be enhanced for both schemes. This is as

<sup>4</sup>The feasible rate can evaluate the suitability of the decoding orders being used. For example, when a strong interference exists at one of the receivers, the receiver cannot directly recover its desired information without using SIC and thus the benchmark scheme may be infeasible/unsuitable.

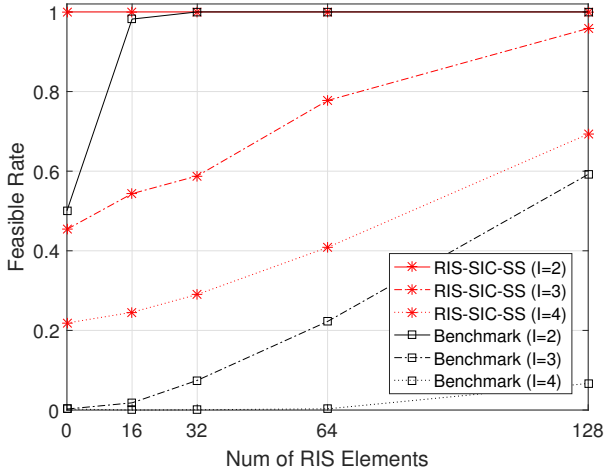


Fig. 3: Comparisons of feasible rate.

expected since RIS can reform the transmitter-RIS-receiver links to focus the energy of the signals and to alleviate interference, which also facilitates the receivers to recover their desired information; 4) With the increase of the number of the transceiver pairs, the feasible rate decreases. This is as expected since the increase of transceiver pairs aggravates the interference, which makes the SINR requirements difficult to be satisfied at the same time.

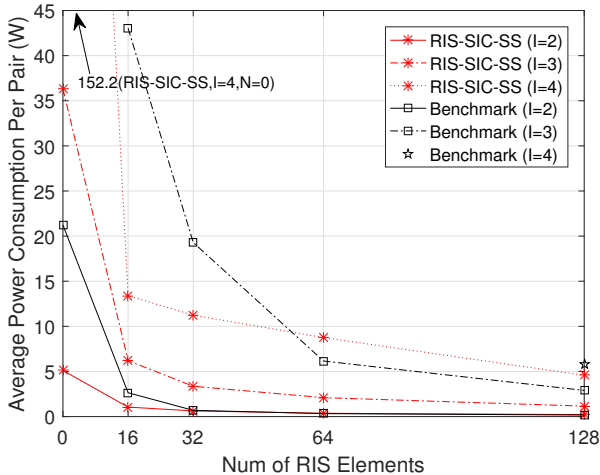


Fig. 4: Comparisons of average power consumption per transceiver pair.

Fig. 4 shows the average power consumption of the proposed RIS-SIC-SS scheme and that of the benchmark scheme, where the results of the benchmark scheme when  $N \leq 64$ ,  $I = 4$  and  $N = 0$ ,  $I = 3$  are not presented because the feasible rates are too small to obtain accurate results. Several observations are drawn as follows: 1) The proposed RIS-SIC-SS scheme can significantly reduce the power consumption. This is because the SIC technique helps alleviate interference such that less signal power is needed; 2) Even without using RIS, the SIC-enabled SSN can still reduce the power consumption;

3) With the increase of the number of RIS elements, the power consumption can be reduced for both schemes. This again validates the effectiveness of RIS when it comes to energy concentration and interference alleviation; 4) The proposed RIS-SIC-SS scheme can support heavier data traffic for given power supply. In particular, the power consumption of the proposed scheme when  $N = 32$ ,  $I = 4$  is even lower than that of the benchmark scheme when  $N = 32$ ,  $I = 3$ .

## V. CONCLUDING REMARKS

For RIS-SSN, this letter proposed to apply the SIC technique to alleviate the interference among different transceiver pairs. A mixed-combinatorial-and-continuous power minimization problem was formulated, in which the decoding order at each receiver, the reflection coefficients at RIS, and the transmit power at each transmitter are jointly optimized under the data rate constraints. To address the problem, a low-complexity but effective decoding order determining method was first proposed. Given the decoding orders, the reflection coefficients and the transmit power were alternatively optimized with the help of the SDR method. Numerical results demonstrated that the proposed RIS-SIC-SS scheme can remarkably improve the feasible rate and reduce the power consumption compared with the benchmark scheme.

## REFERENCES

- [1] J. Lin, W. Yu, N. Zhang, X. Yang, H. Zhang, and W. Zhao, "A survey on Internet of Things: Architecture, enabling technologies, security and privacy, and applications," *IEEE Internet Things J.*, vol. 4, no. 5, pp. 1125–1142, Oct. 2017.
- [2] T. Wang, G. Li, B. Huang, Q. Miao, J. Fang, P. Li, H. Tan, W. Li, J. Ding, J. Li, and Y. Wang, *Spectrum Analysis and Regulations for 5G*. Cham: Springer International Publishing, 2017, pp. 27–50.
- [3] L. Zhang and Y. C. Liang, "Joint spectrum sensing and packet error rate optimization in cognitive IoT," *IEEE Internet Things J.*, vol. 6, no. 5, pp. 7816–7827, Oct. 2019.
- [4] X. Kang, Y. Liang, and J. Yang, "Riding on the primary: A new spectrum sharing paradigm for wireless-powered IoT devices," *IEEE Trans. Wireless Commun.*, vol. 17, no. 9, pp. 6335–6347, Sep. 2018.
- [5] J. Xue, S. Biswas, A. C. Cirik, H. Du, Y. Yang, T. Ratnarajah, and M. Sellathurai, "Transceiver design of optimum wirelessly powered full-duplex MIMO IoT devices," *IEEE Trans. Commun.*, vol. 66, no. 5, pp. 1955–1969, May 2018.
- [6] M. D. Renzo, A. Zappone, M. Debbah, M. S. Alouini, C. Yuen, J. de Rosny, and S. Tretyakov, "Smart radio environments empowered by reconfigurable intelligent surfaces: How it works, state of research, and the road ahead," *IEEE J. Select. Areas Commun.*, vol. 38, no. 11, pp. 2450–2525, Nov. 2020.
- [7] Y. Chen, B. Ai, H. Zhang, Y. Niu, L. Song, Z. Han, and H. V. Poor, "Reconfigurable intelligent surface assisted device-to-device communications," *IEEE Trans. Wireless Commun.*, early access, 2020.
- [8] L. Dai, B. Wang, Z. Ding, Z. Wang, S. Chen, and L. Hanzo, "A survey of non-orthogonal multiple access for 5G," *IEEE Commun. Surveys Tuts.*, vol. 20, no. 3, pp. 2294–2323, thirdquarter 2018.
- [9] M. Cui, G. Zhang, and R. Zhang, "Secure wireless communication via intelligent reflecting surface," *IEEE Wireless Commun. Lett.*, vol. 8, no. 5, pp. 1410–1414, Oct. 2019.
- [10] X. Mu, Y. Liu, L. Guo, J. Lin, and N. Al-Dhahir, "Exploiting intelligent reflecting surfaces in NOMA networks: Joint beamforming optimization," *IEEE Trans. Wireless Commun.*, vol. 19, no. 10, pp. 6884–6898, Oct. 2020.
- [11] M. Fu, Y. Zhou, and Y. Shi, "Intelligent reflecting surface for downlink non-orthogonal multiple access networks," in *IEEE Globecom Workshops*, Dec. 2019, pp. 1–6.
- [12] G. Yang, X. Xu, Y. C. Liang, and M. D. Renzo, "Reconfigurable intelligent surface assisted non-orthogonal multiple access," *IEEE Trans. Wireless Commun.*, early access, 2021.